**Velocity-dependent actomyosin ATPase cycle revealed by *in vitro* motility assay with kinetic analysis**

Masaaki K. Sato[†], Takashi Ishihara[‡], Hiroto Tanaka[§], Akihiko Ishijima[†], and Yuichi Inoue[†]

[†]Institute of Multidisciplinary Research for Advanced Materials, Tohoku University, Aoba-ku, Sendai, 980-8577, Japan.
[‡]Graduate School of Engineering, Nagoya University, Chikusa-ku, Nagoya, 464-8603, Japan
[§]Advanced ICT Research Institute, National Institute of Information and Communications Technology, 588-2, Iwaoka, Nishi-ku, Kobe, 651-2492, Japan

## SUPPORTING MATERIALS

## CONTENTS

**Supporting Table S1. Complete data from this study.** Means ± S.E.

| Applied [HMM] (mg/mL) | Density (HMM/μm$^2$) | [ATP] (μM) | n | Sliding velocity (μm/s) | Actin length (μm) | Average duration time (s) | *N* from band model | *q* (s$^{-1}$) | Estimated *p* (s$^{-1}$) |
|---|---|---|---|---|---|---|---|---|---|
| 0.10 | 633 | 10 | 139 | 0.57±0.029 | 0.39±0.011 | 1.3±0.086 | 7.35 | 11.3 | 9.24 |
| | | 13 | 105 | 0.62±0.029 | 0.32±0.011 | 0.72±0.047 | 6.00 | 14.5 | 11.9 |
| | | 20 | 193 | 0.98±0.032 | 0.52±0.0094 | 0.95±0.053 | 9.78 | 21.4 | 11.7 |
| | | 30 | 151 | 1.2±0.053 | 0.46±0.011 | 0.71±0.053 | 8.66 | 30.5 | 19.0 |
| 0.12 | 760 | 10 | 151 | 0.41±0.015 | 0.45±0.0084 | 2.3±0.15 | 10.2 | 11.3 | 7.24 |
| | | 13 | 126 | 0.51±0.022 | 0.28±0.0058 | 1.3±0.094 | 6.32 | 14.5 | 16.8 |
| | | 20 | 163 | 0.72±0.023 | 0.42±0.0091 | 1.2±0.078 | 9.48 | 21.4 | 13.0 |
| | | 30 | 191 | 1.1±0.037 | 0.42±0.0087 | 0.91±0.071 | 9.64 | 30.5 | 18.4 |
| 0.15 | 945 | 10 | 151 | 0.47±0.028 | 0.44±0.010 | 2.6±0.16 | 12.5 | 11.3 | 5.53 |
| | | 13 | 120 | 0.53±0.018 | 0.33±0.0069 | 1.6±0.12 | 9.47 | 14.5 | 8.69 |
| | | 20 | 156 | 0.83±0.027 | 0.39±0.0085 | 1.7±0.11 | 11.1 | 21.4 | 12.9 |
| | | 30 | 157 | 1.0±0.034 | 0.45±0.0093 | 1.0±0.069 | 12.9 | 30.5 | 14.1 |
| | | 50 | 110 | 1.4±0.035 | 0.29±0.0093 | 0.57±0.039 | 8.28 | 46.2 | 38.5 |
| | | 100 | 133 | 1.7±0.043 | 0.36±0.0084 | 0.65±0.046 | 10.1 | 75.0 | 55.9 |
| | | 250 | 104 | 2.6±0.069 | 0.37±0.0098 | 0.39±0.028 | 10.5 | 120 | 74.0 |
| | | 500 | 102 | 2.9±0.097 | 0.34±0.0080 | 0.28±0.023 | 9.70 | 150 | 103 |
| 0.20 | 1267 | 20 | 141 | 0.77±0.017 | 0.43±0.010 | 2.4±0.15 | 16.2 | 21.4 | 9.20 |
| | | 30 | 160 | 1.1±0.019 | 0.48±0.0092 | 1.6±0.087 | 18.2 | 30.5 | 10.9 |
| | | 50 | 107 | 0.96±0.024 | 0.26±0.0055 | 1.2±0.099 | 9.88 | 46.2 | 36.6 |
| | | 100 | 129 | 1.5±0.036 | 0.42±0.0062 | 0.81±0.054 | 16.0 | 75.0 | 32.7 |
| | | 250 | 148 | 2.6±0.051 | 0.29±0.0052 | 0.54±0.028 | 11.1 | 120 | 86.2 |
| | | 500 | 125 | 2.9±0.054 | 0.46±0.0055 | 0.56±0.029 | 17.4 | 150 | 66.1 |
| 0.25 | 1583 | 20 | 131 | 1.1±0.042 | 0.26±0.0080 | 1.5±0.13 | 12.2 | 21.4 | 10.9 |
| | | 30 | 113 | 1.4±0.036 | 0.36±0.0090 | 0.92±0.062 | 17.0 | 30.5 | 9.69 |
| | | 50 | 121 | 1.5±0.029 | 0.29±0.0060 | 1.1±0.071 | 13.8 | 46.2 | 22.9 |
| | | 100 | 108 | 2.3±0.047 | 0.29±0.0052 | 0.75±0.047 | 13.6 | 75.0 | 38.0 |
| | | 250 | 121 | 2.7±0.057 | 0.30±0.0052 | 0.60±0.035 | 14.3 | 120 | 65.2 |
| | | 500 | 106 | 3.3±0.075 | 0.29±0.0056 | 0.55±0.039 | 13.5 | 150 | 83.5 |
| 0.30 | 1900 | 20 | 141 | 0.54±0.013 | 0.26±0.0049 | 2.1±0.14 | 14.6 | 21.4 | 9.76 |
| | | 30 | 105 | 1.0±0.025 | 0.24±0.0079 | 1.8±0.14 | 13.9 | 30.5 | 15.5 |
| | | 50 | 112 | 1.2±0.029 | 0.27±0.0040 | 0.96±0.063 | 15.1 | 46.2 | 20.3 |
| | | 100 | 121 | 1.8±0.034 | 0.33±0.0048 | 0.91±0.064 | 18.6 | 75.0 | 27.5 |
| | | 250 | 144 | 2.4±0.046 | 0.34±0.0040 | 0.63±0.036 | 19.5 | 120 | 39.5 |
| | | 500 | 132 | 3.1±0.051 | 0.36±0.00050 | 0.56±0.034 | 20.3 | 150 | 53.6 |

**Supporting Figures**

**Figure S1.**

Kinetic Scheme 1 is shown in the main text.

To calculate the combined rate from A-M to M-ATP, the processes of reversible ATP binding and actin dissociation are extracted as:

$$A.M \underset{k_{-T}}{\overset{k_T}{\rightleftarrows}} A.M.ATP \xrightarrow{k_{-A}} M.ATP$$

Differential equations for A-M, A-M-ATP, and M-ATP are expressed as follows.

$$\frac{d[A.M]}{dt} = -k_T[ATP][A.M] + k_{-T}[A.M.ATP] \qquad \text{Eq. 2}$$

$$\frac{d[A.M.ATP]}{dt} = k_T[ATP][A.M] - (k_{-T} + k_{-A})[A.M.ATP] \qquad \text{Eq. 3}$$

$$\frac{d[M.ATP]}{dt} = k_{-A}[A.M.ATP] \qquad \text{Eq. 4}$$

From these equations, and the initial conditions,

$$[\text{A-M}]_{t=0} = 1,\ [\text{A-M-ATP}]_{t=0} = [\text{M-ATP}]_{t=0} = 0,$$

and the relationship,

$$[\text{A-M}] + [\text{A-M-ATP}] + [\text{M-ATP}] = 1,$$

the combined rate from A-M to M-ATP is calculated as,

$$\frac{d[M.ATP]}{dt} = \frac{k_T[ATP]\cdot k_{-A}}{\beta}\left[\exp(-\frac{(\alpha-\beta)t}{2}) - \exp(-\frac{(\alpha+\beta)t}{2})\right] \qquad \text{Eq. 5}$$

where α and β represented

$$\alpha = k_T[ATP] + k_{-A} + k_{-T}$$

$$\beta = \sqrt{-4k_T[ATP]\cdot k_{-A} + (k_T[ATP] + k_{-A} + k_{-T})^2}$$

The average duration of the combined rate from A-M to M-ATP is then calculated as

$$\frac{\int_0^\infty t\cdot\frac{k_T[ATP]\cdot k_{-A}}{\beta}\left[\exp(-\frac{(\alpha-\beta)t}{2}) - \exp(-\frac{(\alpha+\beta)t}{2})\right]dt}{\int_0^\infty \frac{k_T[ATP]\cdot k_{-A}}{\beta}\left[\exp(-\frac{(\alpha-\beta)t}{2}) - \exp(-\frac{(\alpha+\beta)t}{2})\right]dt} = \frac{k_T[ATP] + k_{-A} + k_{-T}}{k_T[ATP]\cdot k_{-A}} \qquad \text{Eq. 6}$$

The total duration from A-M-ADP-Pi to M-ATP (= 1/q) is calculated as the sum of the duration from A-M-ADP-Pi to A-M ($1/k_{-P} + 1/k_{-D}$) and that of the combined rate from A-M to M-ATP.

$$\frac{1}{q} = \frac{1}{k_{-P}} + \frac{1}{k_{-D}} + \frac{k_T[ATP] + k_{-A} + k_{-T}}{k_T[ATP] \cdot k_{-A}} \qquad \text{Eq. 7}$$

Rearrangement of this equation yields Eq. 1 in the main text.

Using 200 $s^{-1}$, 1.2 $\mu M^{-1}s^{-1}$, 500 $s^{-1}$, and 2000 $s^{-1}$ for $k_{-PD}$, $k_T$, $k_{-T}$, and $k_{-A}$, respectively, the $q$ is determined as:

| | $q$ ($s^{-1}$) | |
|---|---|---|
| [ATP] (μM) | $k_{-T}$ | |
| | 500 $s^{-1}$ | 0 $s^{-1}$ |
| 10 | 9.12 | 11.3 |
| 13 | 11.7 | 14.5 |
| 20 | 17.4 | 21.4 |
| 30 | 24.9 | 30.5 |
| 50 | 38.0 | 46.2 |
| 100 | 62.8 | 75.0 |
| 250 | 103 | 120 |
| 500 | 132 | 150 |

**Figure S2. Determination of the density of HMM molecules adsorbed on the coverslip.**

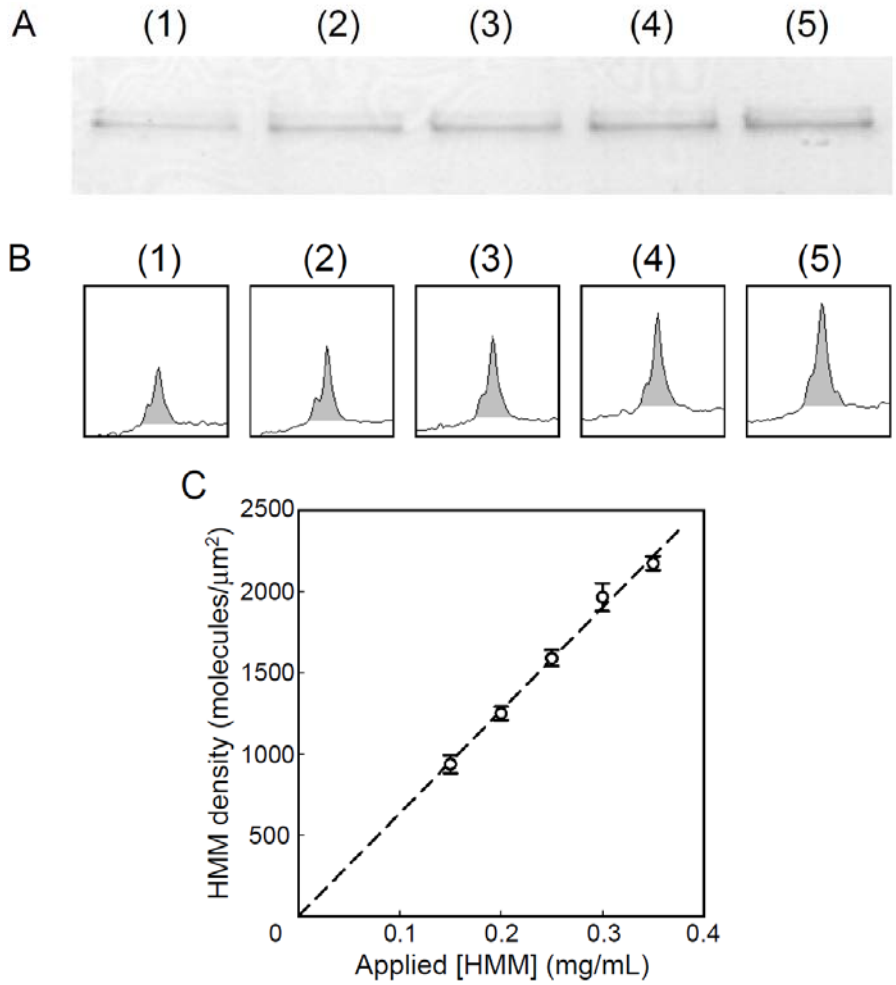


**(A)** CBB staining of the HMM eluted from the flow cells to which was applied (1) 0.15, (2) 0.20, (3) 0.25, (4) 0.30, or (5) 0.35 mg/mL HMM. **(B)** Signal intensities of the bands in (A) quantified by ImageJ. Each intensity (1)-(5) corresponds to the bands in (A) (1)-(5). **(C)** Standard curve between the concentration of applied HMM and the density of HMM on the coverslip. The slope of the standard curve shows:

HMM density (molecules/$\mu m^2$)= 6333 × applied HMM (mg/mL).

Bars indicate S.E. (n = 3).

**Figure S3.**

**Verification that HMM's adsorption on the surface is random.**

To verify that the HMM molecules adhere homogeneously to the surface, tetramethylrhodamine-phalloidine-labeled F-actin which that had been shortened by sonication (mostly <0.5 μm) was loaded into a HMM molecules-adsorbed flow cell under rigor conditions. Fluorescence images were acquired at 20 random areas (Fig. S3A), and the center of mass of each labeled F-actin was measured (Fig. S3B). If HMM molecules were adsorbed on the surface randomly, the labeled F-actin would be observed at random positions. We investigated the randomness by examining (1) the number of labeled F-actin in each picture, (2) autocorrelation among the positions of the labeled F-actin, and (3) the distribution of the nearest neighbor distance of the labeled F-actin.

**(1) The number of labeled F-actin.** The number of labeled F-actin in each picture was 1248 ± 90 (mean ± S.D., n = 20). There was no significant difference in the number of labeled F-actin between images or between the inlet and outlet of the flow cell. We think this is good evidence that the number of HMM molecules adsorbed on the surface was similar in all the areas of the flow cell.

**(2) Autocorrelation among the positions of labeled F-actin in the observed images.** The X- and Y-positions of the labeled F-actin were analyzed by an autocorrelation function (Fig. S3C, D). For both the X- and Y-positions, only a single peak at the origin was observed. This indicates that the HMM molecules were homogeneously adsorbed on the surface, without any periodic crowded regions.

**(3) Distribution of nearest neighbor distance of the labeled F-actin.** To reveal the homogeneity of the adsorption of HMM molecules in more detail, we investigated the nearest neighbor distance (NND) of the labeled F-actin (Fig. S3E). This distribution showed only single peak, as expected for random distribution. The theoretical value of the mean NND <r> was 0.70 ± 0.025 μm ($\langle r \rangle = \frac{1}{2\sqrt{\rho}}$, see Fig. S6). The experimentally obtained <r> was 0.80 ± 0.32 μm (mean ± S.D., n = 24951). The theoretical value and experimentally obtained one were within the acceptable error range. This finding indicates that there is no local region of a higher or lower density of labeled F-actin.

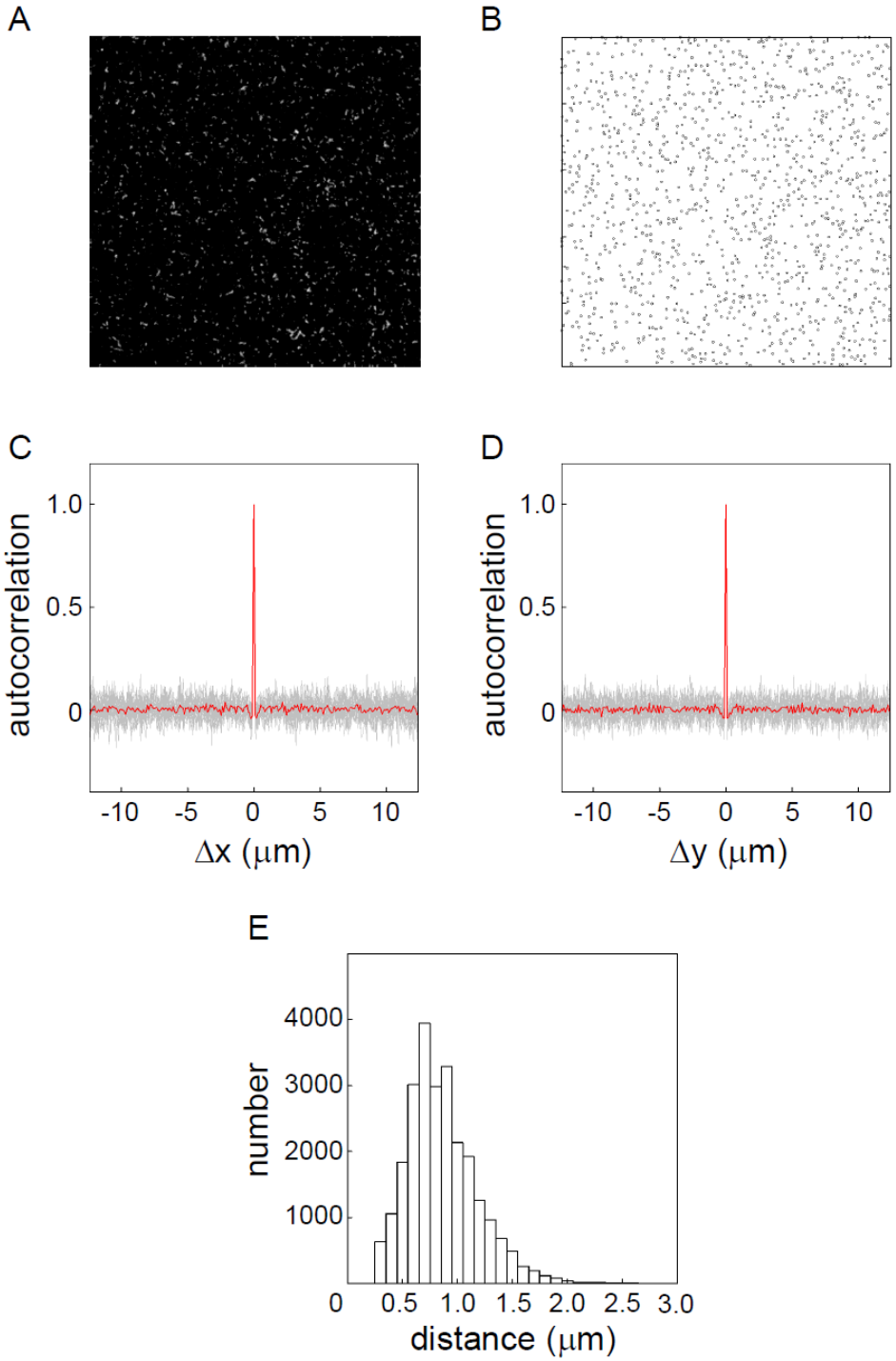


(A) The labeled F-actin in an observed field. The picture size is 49 × 49 μm$^2$. (B) Positions of the center of mass of the labeled F-actin. (C, D) Autocorrelation analysis of the (C) X- and (D) Y-projections of the image in (B). Gray line, individual autocorrelation analysis performed on 20 fields in the flow cell. Red line, the average trace of the autocorrelation analysis. (E) The distribution of the NND of all 20 fields in the flow cell. The total number of positions was 24951.

**Figure S4. Histograms showing the duration of the actomyosin interaction**

**A**

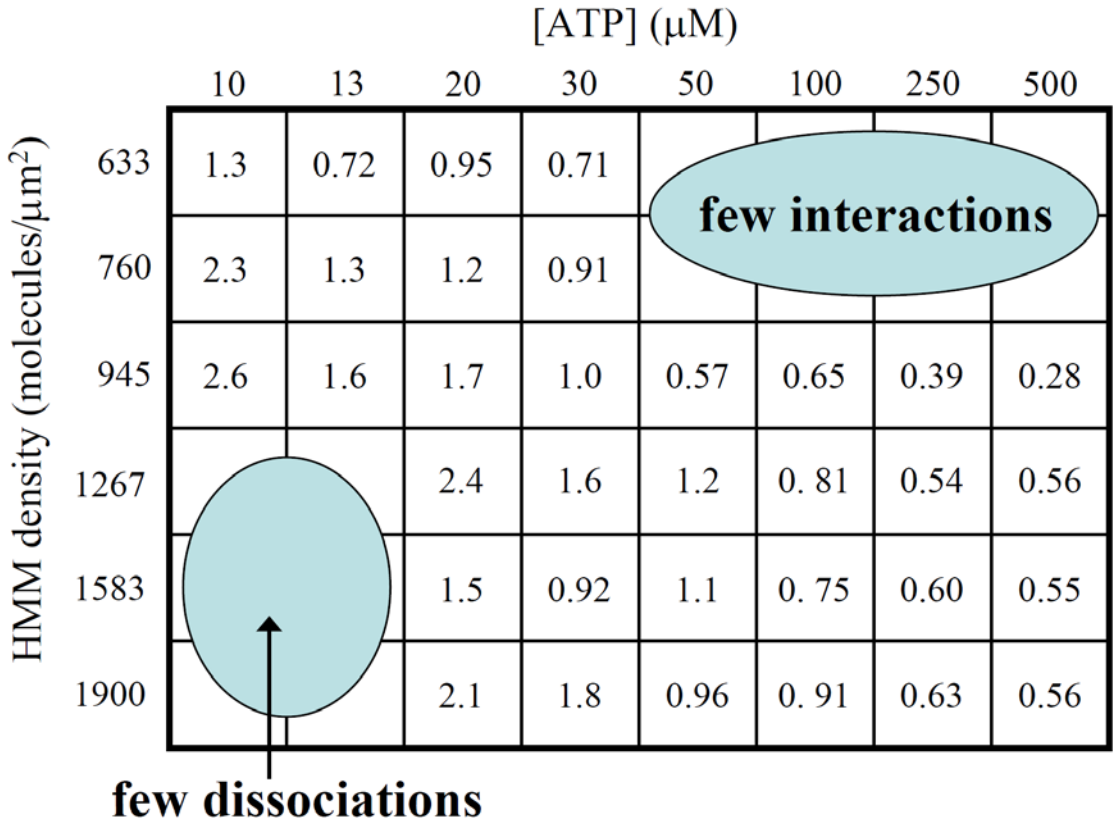


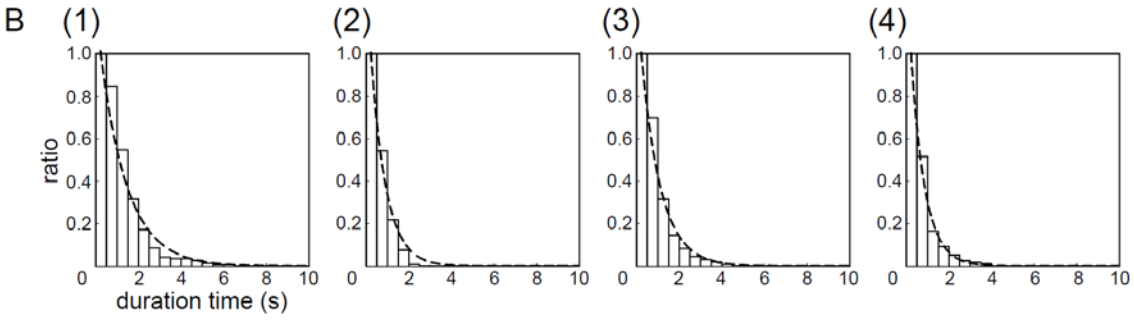


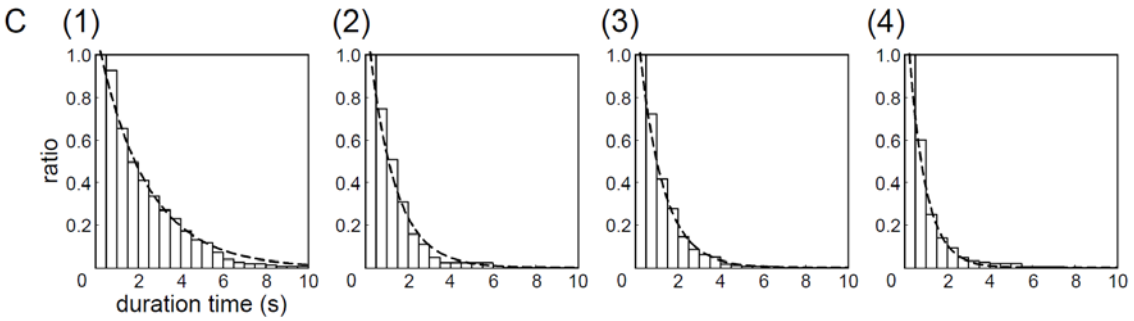

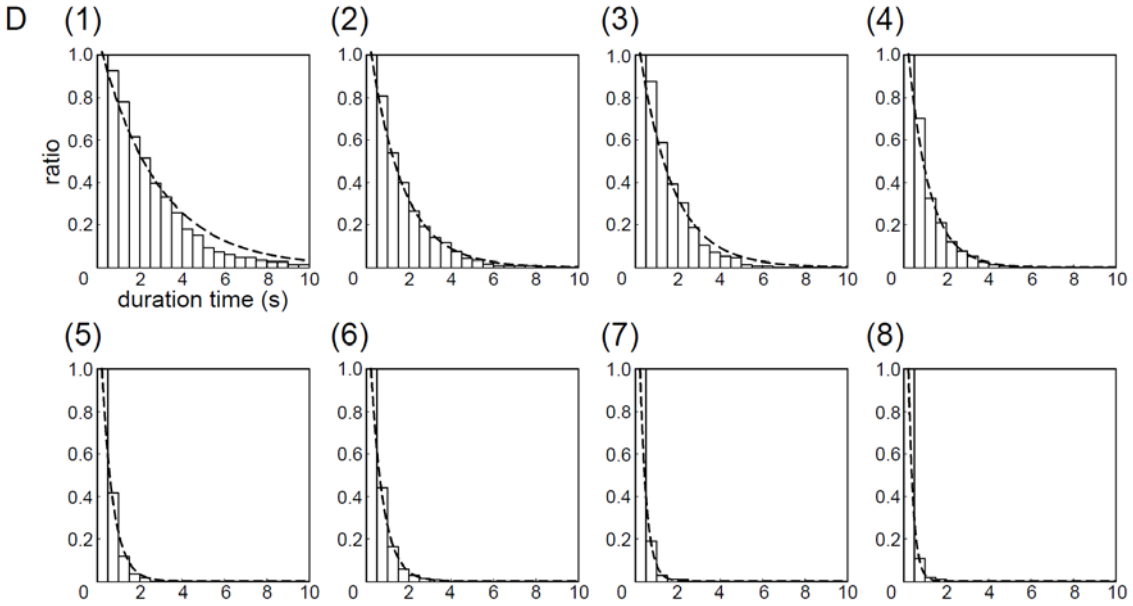
D
(1)
(2)
(3)
(4)
(5)
(6)
(7)
(8)
ratio
duration time (s)

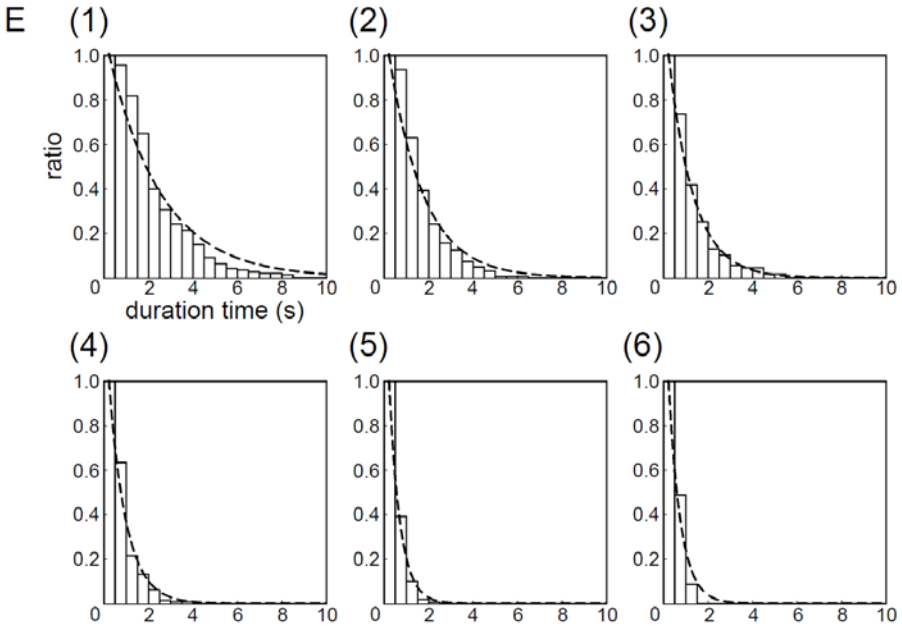
E
(1)
(2)
(3)
(4)
(5)
(6)
ratio
duration time (s)

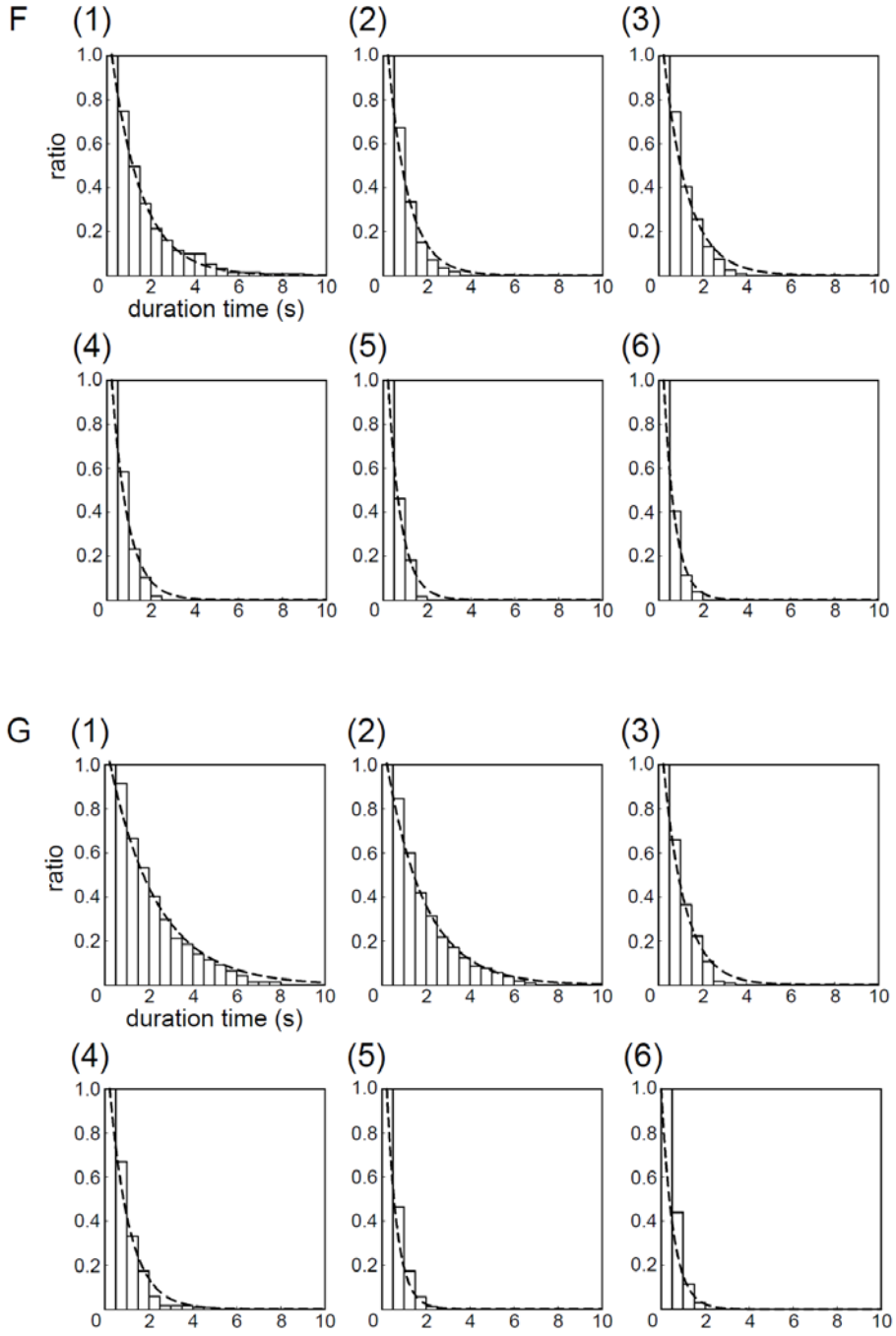


**(A)** Set of experimental conditions. The values in the chart indicate the average sliding duration time for each experimental condition. With 633 and 760 molecules/μm$^2$ and 50-500 μM ATP, few actin filaments attached to HMM. With 1267, 1583, and 1900 molecules/μm$^2$ and 10-13 μM ATP, few actin filaments dissociated from HMM. The duration time of the actomyosin interaction was barely measurable under either of these sets of conditions. **(B)** Histograms for 633 molecules/μm$^2$ with (1) 10 μM, (2) 13

μM, (3) 20 μM, and (4) 30 μM ATP. **(C)** Histograms for 760 molecules/$\mu m^2$ with (1) 10 μM, (2) 13 μM, (3) 20 μM, and (4) 30 μM ATP. **(D)** Histograms for 945 molecules/$\mu m^2$ with (1) 10 μM, (2) 13 μM, (3) 20 μM, (4) 30 μM, (5) 50 μM, (6) 100 μM, (7) 250 μM, and (8) 500 μM ATP. **(E)** Histograms for 1267 molecules/$\mu m^2$ with (1) 20 μM, (2) 30 μM, (3) 50 μM, (4) 100 μM, (5) 250 μM, and (6) 500 μM ATP. **(F)** Histograms for 1583 molecules/$\mu m^2$ with (1) 20 μM, (2) 30 μM, (3) 50 μM, (4) 100 μM, (5) 250 μM, and (6) 500 μM ATP. **(G)** Histograms for 1900 molecules/$\mu m^2$ with (1) 20 μM, (2) 30 μM, (3) 50 μM, (4) 100 μM, (5) 250 μM, and (6) 500 μM ATP. The dotted lines represent the calculation-derived duration time. The total number of observed actin filaments for each panel, n = 102-193.

**Figure S5. Calculation of the duration time using Mathematica**

For example, $N = 2$, $p = q = 0.5$.

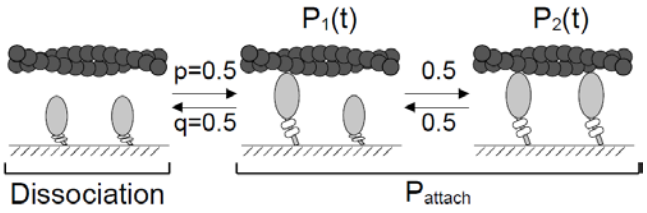


```
nn = Input["nn = ?"]
```
number of cross-bridges

```
2
```

```
pp = Input["pp = ?"]
```
association rate constant

```
0.5
```

```
qq = Input["qq = ?"]
```
dissociation rate constant

```
0.5
```

```
tmax = Input["tmax = ?"]
```

```
10
```

```
var = Table[P[i][t], {i, nn}]
```

```
{P[1][t], P[2][t]}
```

```
(*initial =(Table[P[i][0]==0,{i,nn}] /. P[1][0]==0→ P[1][0]==1)*)
```

```
initial = (Table[P[i][0] == 0, {i, nn}] /. P[nn][0] == 0 → P[nn][0] == 1)
```

```
{P[1][0] == 0, P[2][0] == 1}
```

```
lhs = Table[P[i]'[t], {i, nn}]
```

```
{P[1]'[t], P[2]'[t]}
```

```
rhs =
 Table[(nn - i + 1) p P[i - 1][t] + (i + 1) q P[i + 1][t] - (i q + (nn - i) p) P[i][t], {i, 1, nn}] /.
   P[0][t] → 0 /. P[nn + 1][t] → 0
```

```
{-(p + q) P[1][t] + 2 q P[2][t], p P[1][t] - 2 q P[2][t]}
```

```
Thread[Equal[lhs, rhs]]
```

```
{P[1]'[t] == -(p + q) P[1][t] + 2 q P[2][t], P[2]'[t] == p P[1][t] - 2 q P[2][t]}
```

```
Join[%, initial] /. p → pp /. q → qq
```

```
{P[1]'[t] == -1. P[1][t] + 1. P[2][t],
 P[2]'[t] == 0.5 P[1][t] - 1. P[2][t], P[1][0] == 0, P[2][0] == 1}
```

```
sol = var /. NDSolve[%, var, {t, 0, tmax}][[1]]
```

```
{InterpolatingFunction[{{0., 10.}}, <>][t], InterpolatingFunction[{{0., 10.}}, <>][t]}
```

```
Plot[sol[[1]], {t, 0, tmax}, PlotRange → All, PlotStyle → RGBColor[0, 0, 1]];
```

```
Table[Plot[sol[[i]], {t, 0, tmax}, PlotRange → All, DisplayFunction → Identity], {i, 2, nn}]
```

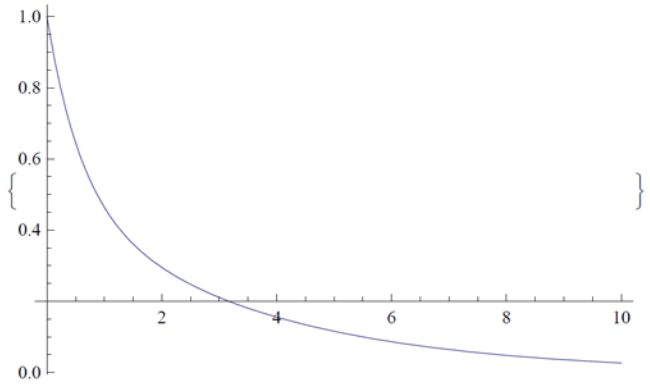


```
Plot[Sum[sol[[i]], {i, nn}], {t, 0, tmax}, PlotRange → All, PlotStyle → RGBColor[1, 0, 0]];

Show[%, %%, %%%]
```

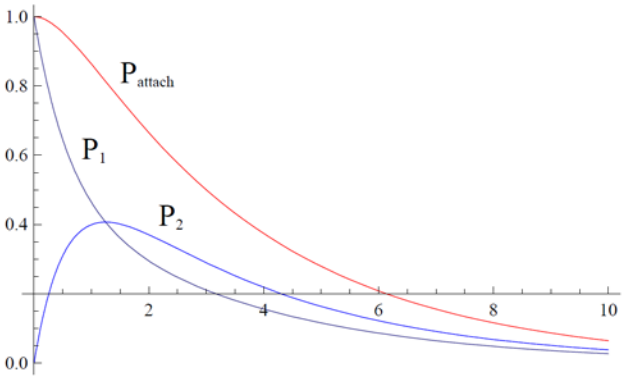


Red line $P_{attach}$ represents the probability that the interaction is maintained.

Blue lines $P_1$ and $P_2$ represent the probability that each state is maintained.

```
Table[Sum[sol[[i]], {i, nn}], {t, 0, tmax, tmax / 20}]
```

```
{1., 0.954458, 0.863057, 0.761934, 0.665143, 0.577516, 0.500113,
 0.432525, 0.373833, 0.323005, 0.279044, 0.241048, 0.208218, 0.179856,
 0.155356, 0.134193, 0.115912, 0.100122, 0.0864825, 0.0747011, 0.0645247}
```

**Figure S6**

**Band model and nearest neighbor distance model.**

**(A)** The band model assumes that HMM molecules (ρ molecules/μm$^2$) inside a certain bandwidth (*w* μm) of both sides of the actin filament (*L* μm in length) can interact with the filament. The predicted number of available cross-bridges *N* is:

$$N = w \cdot \rho \cdot L$$

According to Uyeda et al. (Supporting reference 1), we estimated the *N* with a 30-nm bandwidth, which was derived from electron micrographs of the actin-HMM complex (Supporting reference 2).

**(B)**

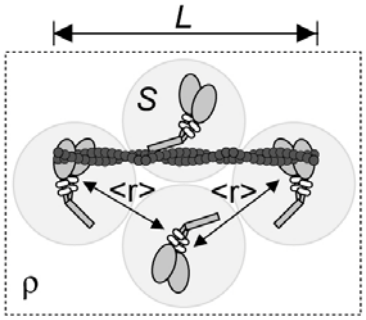


The nearest neighbor distance model assumes that myosin molecules are adsorbed onto the surface following a Poisson distribution. The average number of myosin molecules (*x*) in a certain area (*S*) is:

$$x = \rho \cdot S$$

where ρ is the average density of myosin molecules. Following the Poisson distribution, the distribution of *x* is:

$$P(x) = \frac{(\rho \cdot S)^x}{x!} \cdot \exp(-\rho \cdot \pi r^2)$$

The definition of the nearest neighbor distance is, "the average distance between nearest neighbor particles in randomly distributed ones." Two requirements are needed to satisfy this definition: (1) There is no myosin within a radius r around a myosin located at the center of the circle, (2) There is at least one myosin in an area of (a circle of radius r + dr) - (a circle of radius r).

For requirement (1), $x = 0$ for $S_1 = \pi r^2$,

$$P(0)_1 = \frac{(\rho \cdot \pi r^2)^0}{0!} \cdot \exp(-\rho \cdot \pi r^2)$$

$$= \exp(-\rho \cdot \pi r^2)$$

For requirement (2), $x = 0$ for $S_2 = 2\pi r \cdot dr$, the probability that there is no myosin in $S_2$ is:

$$P(0)_2 = \exp(-\rho \cdot 2\pi r \cdot dr)$$

Then, the probability that there is at least one myosin in $S_2$ is:

$$\begin{aligned} 1 - P(0)_2 &= 1 - \exp(-\rho \cdot 2\pi r \cdot dr) \\ &= 2\pi r \cdot dr \cdot \rho \end{aligned}$$

When both (1) and (2) are satisfied, the following equation is fulfilled:

$$P(r)dr = \exp(-\rho \cdot \pi r^2) \cdot 2\pi r \cdot dr \cdot \rho$$

Thus, the average $r$ is:

$$\langle r \rangle = \int_0^\infty rP(r)dr$$

$$= \int_0^\infty r \cdot 2\pi r \cdot \rho \cdot \exp(-\pi r^2 \rho)dr$$

$$= \frac{1}{2}\sqrt{\frac{1}{\rho}}$$

Therefore, the number of cross-bridges $N$ formed for a single actin filament ($L$) is obtained as:

$$N = \frac{L}{\langle r \rangle}$$

$$= 2\sqrt{\rho} \cdot L$$

To estimate the value of $N$, we adopted the band model. We did not adopt the nearest neighbor distance model, because an important assumption of this model is that "the distance between nearest neighbor particles should be randomly distributed." To fulfill this assumption, it is necessary for the front end of an actin filament to have high flexibility. Considering that the persistence length, the stiffness of an actin filament, and the nearest neighbor distance <$r$> are, respectively, 15 μm (Supporting reference 3), 44 pN/nm (Supporting reference 4), and 11-20 nm (from Fig. S6B and the densities of HMM molecules (633-1900 molecules/μm$^2$)), the actin filaments examined in the present study (0.24-0.52-μm long) are considered to be almost rigid bodies. Therefore, the tip of the actin filaments cannot always interact with the nearest-neighbor HMM molecules, so the number of cross-bridges does not follow this model. Therefore, we decided to use the band model but not the nearest neighbor distance model.

**Figure S7.**

**Estimation of the parameters for the actomyosin interaction.**

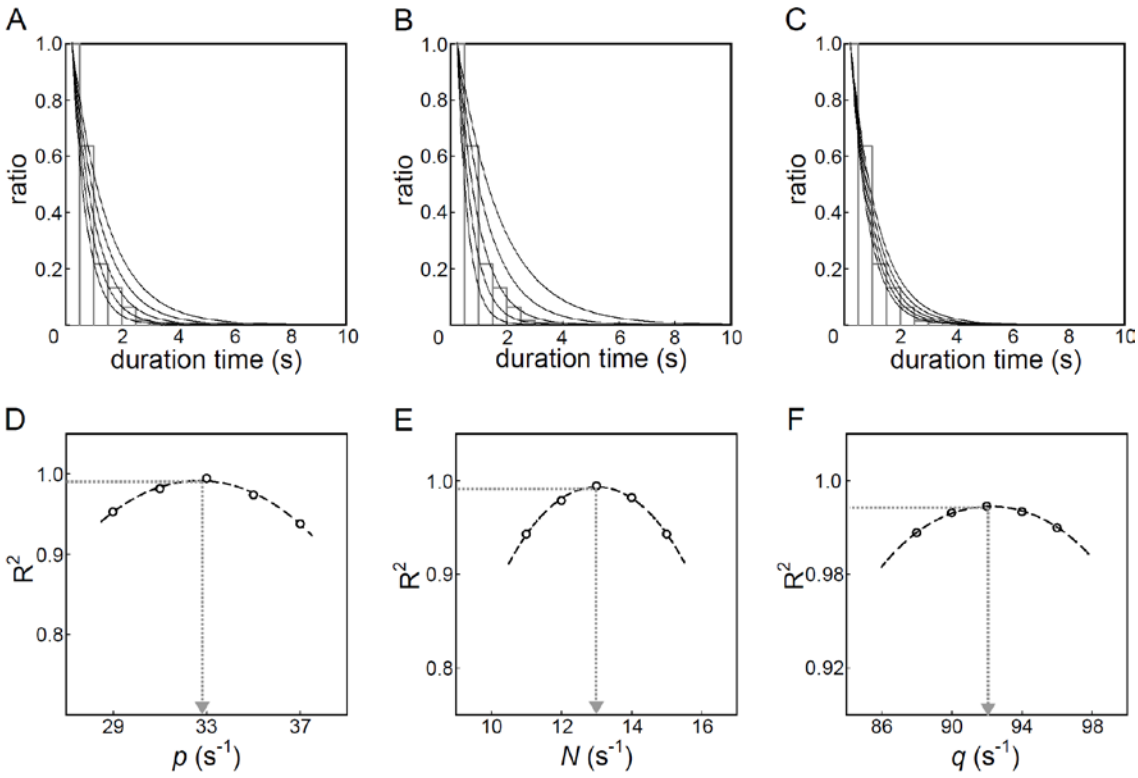


**(A-C)** Experimentally obtained histograms under the condition of 1267 HMM molecules/μm$^2$ and 100 μM ATP, shown with the computationally simulated duration time. **(A)** Determination of the association rate constant *p*. Each duration time was drawn with *N* = 16, *q* = 75, and *p* = 29, 31, 33, 35, 37 (from left to right). **(B)** Determination of the number of cross-bridges *N*. Each duration time was drawn with *p* = 42.4, *q* = 75, and *N* = 11, 12, 13, 14, 15 (from left to right). **(C)** Determination of the dissociation rate constant *q*. Each duration time was drawn with *N* = 16, *p* = 42.4, and *q* = 96, 94, 92, 90, 88 (from left to right).

**(D-F)** Plots of the coefficient of determination $R^2$. The plots were fitted to a Gaussian function. **(D)** Plot of the coefficients of determination $R^2$ against *p* under the conditions of (A). **(E)** The plot of $R^2$ against *N* under the conditions of (B). **(F)** The plot of $R^2$ against *q* under the conditions of (C). We regarded the value with the highest $R^2$ as the kinetic parameter of the actomyosin interaction. From the peak values of the fittings, the obtained values of *p*, *N*, and *q* were 32.7, 13.0, and 92.1, respectively.

**Figure S8.**

**Effect of the estimated number of HMM molecules on the velocity-dependent association.**

Whether the estimated number of HMM molecules had an effect on the velocity-dependence of the association rate constant *p* was examined. We determined whether the velocity-dependent association was maintained when the number of cross-bridges was overestimated compared with the band model-estimated number as follows.

(1) HMM molecules were adsorbed on the surface randomly under a Poisson distribution.

(2) The HMM molecules in the area (actin length in the present study) × (width of the band model, 30 nm) interacted with actin filaments.

(3) The number of cross-bridges was determined by the area and the Poisson distribution.

(4) The Poisson distribution was fitted to a Gaussian function approximately, and the number of cross-bridges was overestimated by σ or 2σ over the band model-estimated number (the values are listed below).

| Applied [HMM] (mg/mL) | Density (HMM/μm$^2$) | [ATP] (μM) | *N* from band model | Estimated *p* (s$^{-1}$) | *N* + σ | Estimated *p* (s$^{-1}$) | *N* + 2σ | Estimated *p* (s$^{-1}$) |
|---|---|---|---|---|---|---|---|---|
| 0.10 | 633 | 10 | 7.35 | 9.24 | 9.85 | 5.55 | 12.6 | 3.83 |
| | | 13 | 6.00 | 11.9 | 8.26 | 7.59 | 10.7 | 4.84 |
| | | 20 | 9.78 | 11.7 | 12.8 | 8.25 | 15.9 | 6.39 |
| | | 30 | 8.66 | 19.0 | 11.4 | 5.82 | 14.4 | 10.8 |
| 0.12 | 760 | 10 | 10.2 | 7.24 | 13.2 | 5.21 | 16.4 | 3.93 |
| | | 13 | 6.32 | 16.8 | 8.63 | 8.98 | 11.1 | 6.83 |
| | | 20 | 9.48 | 13.0 | 12.4 | 10.1 | 15.5 | 7.63 |
| | | 30 | 9.64 | 18.4 | 12.4 | 14.4 | 15.5 | 10.8 |
| 0.15 | 945 | 10 | 12.5 | 5.53 | 15.7 | 4.18 | 19.3 | 3.68 |
| | | 13 | 9.47 | 8.69 | 12.1 | 6.83 | 15.2 | 5.16 |
| | | 20 | 11.1 | 12.9 | 14.1 | 9.44 | 17.4 | 7.56 |
| | | 30 | 12.9 | 14.1 | 16.1 | 10.8 | 19.6 | 8.25 |
| | | 50 | 8.28 | 38.5 | 10.8 | 24.5 | 13.7 | 17.9 |
| | | 100 | 10.1 | 55.9 | 13.1 | 39.1 | 16.3 | 30.0 |
| | | 250 | 10.5 | 74.0 | 13.5 | 59.0 | 16.7 | 42.0 |
| | | 500 | 9.70 | 103 | 12.5 | 80.5 | 15.6 | 55.5 |
| 0.20 | 1267 | 20 | 16.2 | 9.20 | 20.1 | 6.91 | 24.2 | 5.56 |
| | | 30 | 18.2 | 10.9 | 22.3 | 8.56 | 26.5 | 6.76 |
| | | 50 | 9.88 | 36.6 | 12.8 | 25.5 | 15.9 | 19.6 |
| | | 100 | 16.0 | 32.7 | 19.7 | 24.9 | 23.7 | 20.0 |
| | | 250 | 11.1 | 86.2 | 14.1 | 62.0 | 17.4 | 48.5 |
| | | 500 | 17.4 | 66.1 | 21.4 | 51.0 | 25.6 | 39.6 |
| 0.25 | 1583 | 20 | 12.2 | 10.9 | 15.6 | 7.60 | 19.1 | 6.11 |
| | | 30 | 17.0 | 9.69 | 21.0 | 7.50 | 25.1 | 6.09 |
| | | 50 | 13.8 | 22.9 | 17.2 | 18.0 | 20.9 | 13.9 |
| | | 100 | 13.6 | 38.0 | 17.2 | 29.7 | 20.9 | 23.0 |
| | | 250 | 14.3 | 65.2 | 17.8 | 47.5 | 21.5 | 37.1 |
| | | 500 | 13.5 | 83.5 | 17.2 | 65.0 | 20.9 | 50.2 |
| 0.30 | 1900 | 20 | 14.6 | 9.76 | 18.4 | 7.62 | 22.2 | 6.03 |
| | | 30 | 13.9 | 15.5 | 17.1 | 12.0 | 20.8 | 9.39 |
| | | 50 | 15.1 | 20.3 | 19.0 | 15.1 | 23.0 | 12.0 |
| | | 100 | 18.6 | 27.5 | 22.9 | 21.8 | 27.2 | 18.1 |
| | | 250 | 19.5 | 39.5 | 23.5 | 33.7 | 27.9 | 28.1 |
| | | 500 | 20.3 | 53.6 | 24.8 | 41.4 | 29.3 | 34.9 |

The association rate constant $p$ was estimated with the Eq. 1 (in the Main text)-derived dissociation rate constant $q$ and Poisson distribution-estimated number of cross-bridges ($N$+σ, $N$+2σ). The linear relationship was maintained even if the number of cross-bridges was increased to $N$+σ and $N$+2σ (green and blue circles, respectively, in the figure below). Therefore, although the values of the association rate constant $p$ were changed, changing the estimated number of cross-bridges had little effect on our current conclusion that the association rate constant $p$ depends linearly on the sliding velocity.

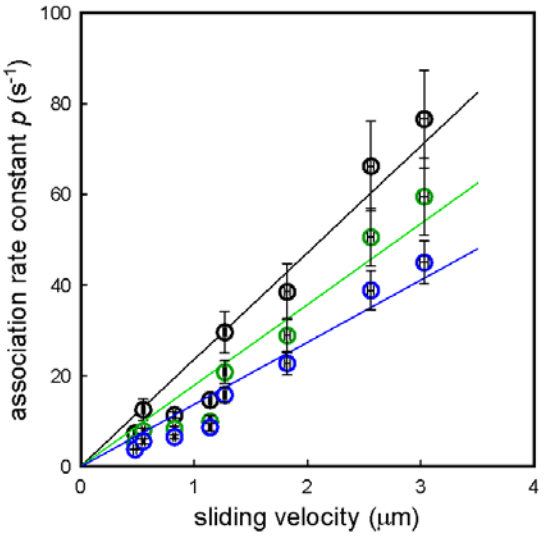


Relationship between the sliding velocity (obtained from Fig. 3E) and the estimated association rate constants. Open black circles, $N$; black slope, 23.5 ± 1.39 (1/s)/(μm/s) (mean ± S.E.). Open green circles, $N$+σ; green slope, 17.8 ± 1.21 (1/s)/(μm/s) (mean ± S.E.). Open blue circles, $N$+2σ; blue slope, 13.7 ± 0.847 (1/s)/(μm/s) (mean ± S.E.). Bars indicate S.E. (for $p$, n = 3-8; for velocity, n = 351-925).

**Figure S9.**

**Estimation of the number of cross-bridges *N* and the dissociation rate constant *q* with a fixed association rate constant *p*.**

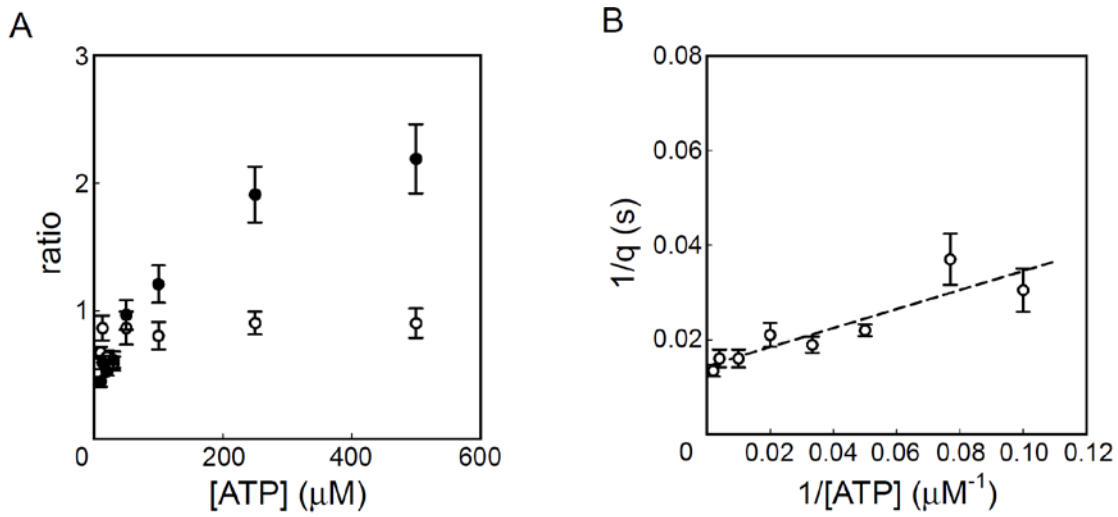


(A) Estimation of *N* using 30 $s^{-1}$ for *p*, 200 $s^{-1}$ for $k_{-PD}$, 1.2 $\mu M^{-1}s^{-1}$ for $k_T$, 0 $s^{-1}$ for $k_{-T}$, and 2000 $s^{-1}$ for $k_{-A}$. The ratio of estimated *N* (molecules/μm) / predicted *N* from the band model (band width = 30 nm), using *p* calculated from the sliding velocity of actin filaments (open circles) and *p* = 30 $s^{-1}$ (closed circles), was plotted against the ATP concentration. Bars indicate S.E. (n = 3-8). (B) Estimation of *q* using 30 $s^{-1}$ and the band model (band width = 30 nm) for *p* and *N*, respectively. Double-reciprocal plot between the estimated *q* and the ATP concentration. Bars indicate S.E. (n = 3-8). The slope and the y-intercept were 0.201 ± 0.0400 μM·s and 0.0144 ± 0.00200 s, respectively (means ± S.E.). The coefficient of determination $R^2$ of the fitted line was 0.808.

**Supporting Movies**

The motion of actin filaments was video-recorded. The picture size of Movie S1-S4 is 6 × 6 μm.

**Movie S1**

An actin filament sliding, under the following conditions: 945 HMM molecules/$\mu m^2$ and 30 μM ATP.

**Movie S2**

An actin filament sliding under the following conditions: 945 HMM molecules/$\mu m^2$ and 500 μM ATP.

**Movie S3**

An actin filament sliding under the following conditions: 1267 HMM molecules/$\mu m^2$ and 30 μM ATP.

**Movie S4**

An actin filament sliding under the following conditions: 1267 HMM molecules/$\mu m^2$ and 500 μM ATP.

**Supporting References**

1. Uyeda, T. Q. P., S. J. Kron, and J. A. Spudich. 1990. Myosin step size estimation from slow sliding movement of actin over low densities of heavy meromyosin. *J. Mol. Biol.* 214:699-710.

2. Toyoshima, Y. Y., C. Toyoshima, and J. A. Spudich. 1989. Bidirectional movement of actin filaments along tracks of myosin heads. *Nature* 341:154-156.

3. Yanagida, T., M. Nakase, K. Nishiyama, and F. Oosawa. 1984. Direct observation of myosin of single F-actin filaments in the presence of myosin. *Nature* 307:58-60.

4. Kojima, H., A. Ishijima, and T. Yanagida. 1994. Direct measurement of stiffness of single actin filaments with and without tropomyosin by *in vitro* nanomanipulation. *Proc. Natl. Acad. Sci. USA* 91:12962-12966.